Proceedings of the ASME 2010 3rd Joint US-European Fluids Engineering Summer Meeting and 8th International Conference on Nanochannels, Microchannels, and Minichannels
FEDSM-ICNMM2010
August 1-5, 2010, Montreal, Canada

FEDSM-ICNMM2010-30014

NUMERICAL SIMULATION OF PARTICLE DISPERSION BEHAVIOR UNDER THE REDUCED GRAVITY CONDITIONS

Xue LIU
Harbin Power Equipment Performance Test Center, Harbin Power System Engineering and Research Institute, Harbin, Heilongjiang, China

Guohui LI
School of Electronic and Information Engineering, Dalian Jiaotong University Dalian, Liaoning, China

Yang LIU†
Marine Engineering College, Dalian Maritime University Dalian, Liaoning, China

ABSTRACT

An Euler-Euler two-fluid model based on the second-order-moment closure approach and the granular kinetic theory of dense gas-particle flows was presented. Anisotropy of gas-solid two-phase stress and the interaction between two-phase stresses are fully considered by two-phase Reynolds stress model and the transport equation of two-phase stress correlation. Under the microgravity space environments, hydrodynamic characters and particle dispersion behaviors of dense gas-particle turbulence flows are numerically simulated. Simulation results of particle concentration and particle velocity are in good agreement with measurement data under earth gravity environment. Decreased gravity can decrease the particle dispersion and can weaken the particle-particle collision as well as it is in favor of producing isotropic flow structures. Moreover, axial-axial fluctuation velocity correlation of gas and particle in earth gravity is approximately 3.0 times greater than those of microgravity and it is smaller than axial particle velocity fluctuation due to larger particle inertia and the larger particle turbulence diffusions.

INTRODUCTION

Dense gas-particle turbulence flow plays an important role in particle transportation, chemical process and clean combustion application etc. it is important for us to clearly understand the mechanism of particle-fluid system under microgravity space environments for human beings to explore the potential deep space energy resources[1-6].Microgravity environment can be obtained by the ground-based falling tower test, but it limited to the expensive expenditure, too short falling time and complicated accurate measurement approach. Therefore, numerical simulation technology to predict hydrodynamics of particle-fluid system under microgravity conditions is very importance. Certainly, validation must be performed by ground-based test under earth gravity. Compared with the up-flow fast fluidized bed riser, downer reactors of fluidized bed have many advantages such as good gas-solids contact, less gas and solids back-mixing, a short contact time and more uniform residence time distribution[7-17]. Computational fluid dynamics (CFD) with an Euler-Euler two-fluid modeling approaches has been widely used to predict hydrodynamics in circulated fluidized bed.

Since the particle-particle collision is of great importance in two-phase turbulence flows, the constitutive relation for particle-particle collision are obtained from the kinetic theory of granular flow proposed by Lun and Savage[18]and Ding and Gidaspow[19]. It is similar to an analogy between the dense-gas kinetic theory and the particle random fluctuation due to particle collision, where transfer of particle momentum and produces particle pressure and viscosity are produced. Particle pressure and particle viscosity depend on the magnitude of small-scale particle fluctuations, which can be described by particle thermal energy from particle stress and dissipation through particles inelastic collisions. Savage and Gidaspow[20,21] presented the full equations of kinetic theory for granular flows. Sinclair and Jackson [22] firstly applied it to build a laminar gas-phase and laminar particle-phase model for simulating fully developed flow in vertical pipes. Considering effects of gas turbulence, Bolio and Yasuna[23] accounted for both gas turbulence using k-ε model and particle fluctuation due to particle collisions. Lu et al.[24,25]simulate the gas-particle flow in riser reactors using the kinetic theory, in which the gas turbulence is modeled using large eddy simulation. All of these studies considered that the particle flow is laminar

flow and is not turbulence flow. Thus, large-scale fluctuation from particle turbulence is neglected. So, Zhou et al.[26-28]and Liu and Zhou[29] proposed a k-ε-k_p model, a SGS-USM model to simulate sudden expansion gas-particle turbulence flows. This model can fully consider both the anisotropy of gas-solid two-phase stresses and the interaction between two-phase stresses using two-phase Reynolds stress model using two-phase Reynolds stress incorporated with the transport equation of two-phase stress correlation correlations. Cheng and Guo[30] proposed a k-ε-k_p-Θ dense gas-particle two-phase flow four equation model. Those of simulated results are well agreed with experimental data, which demonstrates this idea is reasonable for small-scale fluctuations due to particle-particle collision and large-scale fluctuations due to particle turbulence.

To date, particle dispersion behaviors in downer under microgravity environments have never been reported. In this paper, an Euler-Euler two-fluid model based on the second-order-moment closure approach and kinetic theory of granular flows of dense gas-particle flows was used to study the hydrodynamic characters of dense gas-particle flows under microgravity conditions.

2. CONSERVATION EQUATIONS OF TWO-PHASE TURBULENCE FLOWS

In the framework of two-fluid model, the conservation equations of two-phase turbulence flows with constitutive and closure relations are as follows.

2.1 Continuity and moment equations

The continuity equations for gas (k=gas) and particle (k=particle) are:

$$\frac{\partial}{\partial t}\left(\alpha_k \rho_k\right)+\frac{\partial}{\partial x_j}\left(\alpha_k \rho_k \overline{u_{ki}}\right)=0 \tag{1}$$

where α_k is the volume fraction of phase k, u_{ki} the velocity vector of phase k, and ρ_k the density of phase k.

The momentum balance equation for the gas phase and particle phase are:

$$\begin{aligned}&\frac{\partial\left(\alpha_g \rho_g \overline{u_{gi}}\right)}{\partial t}+\frac{\partial\left(\alpha_g \rho_g \overline{u_{gk} u_{gi}}\right)}{\partial x_k}=\mathrm{S}_g-\alpha_g \frac{\partial \overline{p}}{\partial x_i}+\\&\frac{\partial}{\partial x_k}\left(\tau_{gik}-\alpha_g \rho_g \overline{u'_{gi} u'_{gk}}\right)-\beta\left(\overline{u_{gi}}-\overline{u_{si}}\right)\end{aligned} \tag{2}$$

$$\begin{aligned}&\frac{\partial\left(\alpha_p \rho_p \overline{u_{si}}\right)}{\partial t}+\frac{\partial\left(\alpha_p \rho_p \overline{u_{pk} u_{pi}}\right)}{\partial x_k}=\mathrm{S}_p-\alpha_p \frac{\partial \overline{p}}{\partial x_i}-\\&\frac{\partial \overline{p_p}}{\partial x_i}+\frac{\partial}{\partial x_k}\left(\tau_{pik}-\alpha_p \rho_p \overline{u'_{pk} u'_{pi}}\right)+\beta\left(\overline{u_{gi}}-\overline{u_{pi}}\right)\end{aligned} \tag{3}$$

Where $\mathrm{S_g}=\alpha_g\rho_g g$ and $\mathrm{S_p}=\alpha_p\rho_p g$ is the gravity source term for gas and particle phase, g is the gravity acceleration, p the thermodynamic pressure, β the interface momentum transfer coefficient, respectively. τ_g and τ_p are gas phase and particle phase viscous stress tensor, their closure are

2.2 Interphase moment exchange

Coupling of momentum transfer between gas and particle phases, a reasonable drag force model is required. When porosities is less than 0.8, the pressure drop due to friction between gas and particles can be described by the Ergun equation. When porosity is greater than 0.8, Wen and Yu[31] equation was used:

$$\beta=150\frac{\alpha_p^2\mu_g}{\alpha_g d_p^2}+1.75\frac{\alpha_p\rho_g\left|\vec{u}_g-\vec{u}_s\right|}{d_p} \qquad \alpha_g<0.8 \tag{4}$$

$$\beta=\frac{3}{4}C_D\frac{\alpha_p\rho_g\left|\vec{u}_g-\vec{u}_p\right|}{d_p}\alpha_g^{-2.65} \qquad \alpha_g\geq 0.8 \tag{5}$$

$$C_D=\frac{24}{\mathrm{Re}_p}\left(1+0.15\,\mathrm{Re}_p^{0.687}\right) \qquad \mathrm{Re}_p\leq 1000 \tag{6}$$

$$C_D=0.44 \qquad \mathrm{Re}_p>1000 \tag{7}$$

$$\mathrm{Re}_p=\frac{\alpha_g\rho_g d_p\left|\vec{u}_g-\vec{u}_s\right|}{\mu_g} \tag{8}$$

2.3 Reynolds stress equations of gas and particle phase

The gas Reynolds stress equation is

$$\begin{aligned}&\frac{\partial\left(\alpha_g\rho_g\overline{u'_{gi}u'_{gj}}\right)}{\partial t}+\frac{\partial\left(\alpha_g\rho_m\overline{u_{gk}}\cdot\overline{u'_{gi}u'_{gj}}\right)}{\partial x_k}=D_{g,ij}+\\&P_{g,ij}+\Pi_{g,ij}-\varepsilon_{g,ij}+G_{g,gp,ij}\end{aligned} \tag{9}$$

where the terms on the right-hand side of Eq.9 stand for the diffusion term, shear production term, pressure-strain term, dissipation term and gas-particle interaction term, respectively. They are closed as follows:

$$D_{g,ij}=\frac{\partial}{\partial x_k}\left(C_g\alpha_g\rho_g\frac{k_g}{\varepsilon_g}\overline{u'_{gk}u'_{gl}}\frac{\partial\overline{u'_{gi}u'_{gj}}}{\partial x_l}\right) \tag{10}$$

$$P_{g,ij}=-\alpha_g\rho_g\left(\overline{u'_{gk}u'_{gj}}\frac{\partial\overline{u_{gi}}}{\partial x_k}+\overline{u'_{gk}u'_{gi}}\frac{\partial\overline{u_{gj}}}{\partial x_k}\right) \tag{11}$$

$$\begin{aligned}&\Pi_{g,ij}=\Pi_{g,ij,1}+\Pi_{g,ij,2}=-C_{g1}\frac{\varepsilon_g}{k_g}\alpha_g\rho_g\\&\left(\overline{u'_{gi}u'_{gj}}-\frac{2}{3}k_g\delta_{ij}\right)-C_{g2}\left(P_{g,ij}-\frac{2}{3}P_g\delta_{ij}\right)\end{aligned} \tag{12}$$

$$P_g=-\alpha_g\rho_g\overline{u'_{gk}u'_{gi}}\frac{\partial\overline{u_{gi}}}{\partial x_k} \tag{13}$$

$$G_{g,gp,ij}=\beta\left(\overline{u'_{pi}u'_{gj}}+\overline{u'_{gi}u'_{pj}}-2\overline{u'_{gi}u'_{gj}}\right) \tag{14}$$

The particle Reynolds stress equation is

$$\frac{\partial\left(\alpha_p\rho_p\overline{u'_{pi}u'_{pj}}\right)}{\partial t}+\frac{\partial\left(\alpha_p\rho_{sm}\overline{u_{pk}}\cdot\overline{u'_{pi}u'_{pj}}\right)}{\partial x_k}=D_{p,ij}+ \quad (15)$$

$$P_{p,ij}+\Pi_{p,ij}-\varepsilon_{p,ij}+G_{p,gp,ij}$$

where the terms on the right-hand side of Eq.15 stand for the diffusion term, shear production term, pressure-strain term, dissipation term and gas-particle interaction term, respectively. They are closed as follows:

$$D_{p,ij}=\frac{\partial}{\partial x_k}\left(C_s\alpha_p\rho_p\frac{k_p}{\varepsilon_p}\overline{u'_{pk}u'_{pl}}\frac{\partial\overline{u'_{pi}u'_{pj}}}{\partial x_l}\right) \quad (16)$$

$$P_{p,ij}=-\alpha_{\mathrm{p}}\rho_{pm}\left(\overline{u'_{pk}u'_{pj}}\frac{\partial\overline{u_{pi}}}{\partial x_k}+\overline{u'_{pk}u'_{pi}}\frac{\partial\overline{u_{pj}}}{\partial x_k}\right) \quad (17)$$

$$\Pi_{p,ij}=\Pi_{p,ij,1}+\Pi_{p,ij,2}=-C_{p1}\frac{\varepsilon_p}{k_p}\alpha_p\rho_p \quad (18)$$

$$\left(\overline{u'_{pi}u'_{pj}}-\frac{2}{3}k_p\delta_{ij}\right)-C_{p2}\left(P_{p,ij}-\frac{2}{3}P_p\delta_{ij}\right)$$

$$\varepsilon_{p,ij}=\frac{2}{3}\delta_{ij}\alpha_{\mathrm{p}}\rho_p\varepsilon_p \quad (19)$$

$$G_{p,gp,ij}=\beta\left(\overline{u'_{pi}u'_{gj}}+\overline{u'_{pj}u'_{pi}}-2\overline{u'_{pi}u'_{pj}}\right) \quad (20)$$

For dense gas-particle flows, pressure-strain term and dissipation term caused by particle pressure P_p and particle viscosity shear stress $\varepsilon_{p,ij}$ for particle-particle collision. The redistribution and dissipation of particle Reynolds stress in every direction are produced. Thus, particle temperature is incorporated into second-order-moment model.

2.4 Dissipation transport equations of turbulent kinetic energy

Dissipation transport equations of turbulent kinetic energy for gas and particle phase are:

$$\frac{\partial\left(\alpha_g\rho_g\varepsilon_g\right)}{\partial t}+\frac{\partial\left(\alpha_g\rho_g\overline{u_{gk}}\varepsilon_g\right)}{\partial x_k}=\frac{\partial}{\partial x_k}\left(C_g\alpha_g\rho_g\frac{k_g}{\varepsilon_g}\overline{u'_{gk}u'_{gl}}\frac{\partial\varepsilon_g}{\partial x_l}\right) \quad (21)$$

$$+\frac{\varepsilon_g}{k_g}\left[c_{\varepsilon1}\left(P_g+G_{g,gp}\right)-c_{\varepsilon2}\alpha_g\rho_g\varepsilon_g\right]$$

$$\frac{\partial\left(\alpha_p\rho_p\varepsilon_p\right)}{\partial t}+\frac{\partial\left(\alpha_p\rho_p\overline{u_{pk}}\varepsilon_p\right)}{\partial x_k}=\frac{\partial}{\partial x_k}\left(\alpha_p\rho_pC_p^d\frac{k_p}{\varepsilon_p}\overline{u'_{pk}u'_{pl}}\frac{\partial\varepsilon_p}{\partial x_l}\right) \quad (22)$$

$$+\frac{\varepsilon_p}{k_p}\left[C_{\varepsilon p,1}\left(P_p+G_{p,gp}\right)-C_{\varepsilon p,2}\alpha_p\rho_p\varepsilon_p\right]$$

where

$$P_g=-\alpha_g\rho_g\overline{u'_{gk}u'_{gi}}\frac{\partial\overline{u_{gi}}}{\partial x_k} \quad (23)$$

$$P_p=-\varepsilon_p\rho_p\overline{u'_{pi}u'_{pk}}\frac{\partial\overline{u_{pi}}}{\partial x_k} \quad (24)$$

As for the interaction correlation term of gas-particle turbulence, Zhou and Chen[27] established the simply closed correlations using a non-dimensional analysis, and kinetic energy is always greater than zero. But, it is found that it always smaller than gas and particle kinetic energy in many experiments. That is it means the negative existing. Therefore, it is reasonable that this term will be dealt with a turbulence dissipation term for gas-particle phase. Mohanarangam and Tu[32] proposed the correlation transportation equation based on the isotropic turbulence kinetic energy (scalar quantity). Only the shortcoming is that the closed transportation equation cannot reflect the anisotropic turbulence flows. In this study, interaction correlation term indicating anisotropic gas-particle two-phase turbulence flows can be modeled by the following transport equation:

$$\frac{\partial\overline{u'_{pi}u'_{gj}}}{\partial t}+\left(\overline{u_{gk}}+\overline{u_{pk}}\right)\frac{\partial\overline{u'_{pi}u'_{gj}}}{\partial x_k}=D_{g,p,ij} \quad (25)$$

$$+P_{g,p,ij}+\Pi_{g,p,ij}-\varepsilon_{g,p,ij}+T_{gp,ij}$$

where the terms on the right-hand side of Eq.(25) stand for the diffusion term, shear production term, pressure-strain term, dissipation term and gas-particle interaction term, respectively. They are closed as follows

$$D_{g,p,ij}=\frac{\partial}{\partial x_k}\left(C_{gp3}\left(\frac{k_p}{\varepsilon_p}\overline{u'_{pk}u'_{pl}}+\frac{k_g}{\varepsilon_g}\overline{u'_{gk}u'_{gl}}\right)\frac{\partial\overline{u'_{gi}u'_{pj}}}{\partial x_l}\right) \quad (26)$$

$$P_{g,p,ij}=-\overline{u'_{pi}u'_{gk}}\frac{\partial\overline{u_{gj}}}{\partial x_k}-\overline{u'_{pk}u'_{gj}}\frac{\partial\overline{u_{pi}}}{\partial x_k} \quad (27)$$

$$P_{g,p}=-\frac{1}{2}\left(\overline{u'_{pi}u'_{gk}}\frac{\partial\overline{u_{gi}}}{\partial x_k}+\overline{u'_{pk}u'_{gi}}\frac{\partial\overline{u_{pi}}}{\partial x_k}\right) \quad (28)$$

$$\Pi_{g,p,ij}=\Pi_{g,p,ij,1}+\Pi_{g,p,ij,2}=-\frac{C_{g,p,1}}{\tau_{rp}} \quad (29)$$

$$\left(\overline{u'_{pi}u'_{gj}}-\frac{2}{3}k_{g,p}\delta_{ij}\right)-C_{g,p,2}\left(P_{g,p,ij}-\frac{2}{3}P_{g,p}\delta_{ij}\right)$$

$$T_{gp,ij}=\frac{\beta}{\alpha_g\rho_g\alpha_p\rho_p} \quad (30)$$

$$\left[\alpha_p\rho_p\overline{u'_{pi}u'_{pj}}+\alpha_g\rho_g\overline{u'_{gi}u'_{gj}}-\left(\alpha_g\rho_g+\alpha_p\rho_p\right)\overline{u'_{gj}u'_{pi}}\right]$$

$$\varepsilon_{g,p,ij} = \frac{\overline{u'_{pi}u'_{gj}}}{\min\left(\tau_{rp}, k/\varepsilon\right)} \tag{31}$$

2.5 Particle temperature equations with frictional stress model

The conservation equation of particle fluctuating energy or translational granular temperature is

$$\frac{3}{2}\left[\frac{\partial\left(\alpha_p\rho_p\theta\right)}{\partial t}+\frac{\partial\left(\alpha_p\rho_p\overline{u_{pk}}\theta\right)}{\partial x_k}\right]=\frac{\partial}{\partial x_k}\left(C_p\alpha_p\rho_p\frac{k_p^2}{\varepsilon_p}\right)+$$
$$\frac{\partial}{\partial x_k}\left(\Gamma_p\frac{\partial\theta}{\partial x_k}\right)+\mu_p\left(\frac{\partial\overline{u_{pk}}}{\partial x_i}+\frac{\partial\overline{u_{pi}}}{\partial x_k}\right)\frac{\partial\overline{u_{pi}}}{\partial x_k} \tag{32}$$
$$+\mu_p\varepsilon_p-\overline{p_p}\frac{\partial\overline{u_{pl}}}{\partial x_l}+\left(\xi_p-\frac{2}{3}\mu_p\right)\left(\frac{\partial\overline{u_{pl}}}{\partial x_l}\right)^2-\gamma_p$$

where k_p is the conductivity coefficient of granular temperature, it is as follows

$$k_p=\frac{150}{384(1+e)g_0}\rho_p d_p\sqrt{\pi\theta}$$
$$\left[1+\frac{6}{5}(1+e)g_0\alpha_p\right]^2+2\alpha_p^2\rho_p d_p g_0(1+e)\sqrt{\frac{\theta}{\pi}} \tag{33}$$

The translational fluctuation energy dissipation rate is

$$\gamma_p=3\left(1-e^2\right)\alpha_p^2\rho_p g_0\theta\left[\frac{4}{d_p}\sqrt{\frac{\theta}{\pi}}-\frac{\partial u_{pk}}{\partial x_k}\right] \tag{34}$$

The bulk solids viscosity is

$$\xi_p=\frac{4}{3}\alpha_p^2\rho_p d_p g_0(1+e)\sqrt{\frac{\theta}{\pi}} \tag{35}$$

The radial distribution function g_0, can be seen as a measure for the probability of inter-particle correlation

$$g_0=[1-(\frac{\alpha_p}{\alpha_{p,\max}})^{\frac{1}{3}}]^{-1} \tag{36}$$

Where d_p is the particle diameter, e the coefficient of particle restitution, $\varepsilon_{p,max}$ is the particle maximum volume fraction at random packing.

The particle pressure represents the particle normal forces due to particle-particle interaction. It is calculated as follows

$$P_p=\alpha_p\rho_p[1+2(1+e)\alpha_p g_0]\theta \tag{37}$$

The equation of particle viscosity can be expressed as a function of granular temperature of the following equations

$$\mu_p=\frac{2\mu_{p,dil}}{(1+e)g_0}\left[1+\frac{4}{5}(1+e)g_0\alpha_p\right]^2+$$
$$\frac{4}{5}\alpha_p^2\rho_p d_p g_0(1+e)\sqrt{\frac{\theta}{\pi}} \tag{38}$$

$$\mu_{p,dil}=\frac{5}{96}\rho_p d_p\sqrt{\pi\theta} \tag{39}$$

2.6 Boundary conditions and experiments

For boundary conditions, at the inlet, particle with a flat uniform velocity profile and air with a parabolic velocity profile are set. All velocity and volume fraction of both phase were specified. Averaged inlet superficial gas phase velocity is 4.33m/s. Particle volume fraction is 0.02. The normal components of Reynolds stresses are assumed to have an isotropic inlet distribution and the shear stresses are determined by eddy viscosity expressions. The turbulent kinetic energy and its dissipation rate are taken by empirical expressions. At the outlet, the fully developed flow conditions of two-phase are taken. At the wall, no slip condition is used for gas phase velocity and gas Reynolds stress are determined via production term including the effect of wall function for near wall grid nodes. $\frac{\partial\varphi}{\partial x}=0\left(\varphi=u_{g,p},v_{g,p},u'_{g,p},.....\right)$. Particle phase used a partial slip condition considering the wall roughness[11]. At the near-wall grid nodes, the wall-function approximation is used. At the axis, symmetric conditions are adopted for both the two phase. The convergence criteria for gas and particle phase are mass source 5.0×10^{-5}.

Measured data by Wang et al.[33] is used to validate the simulation results under earth gravity environment. The downer is 5.8m high with as diameter of 0.14 m. Averaged gas inlet velocity is 4.33 m/s and particles flow rates is Gs=65 kg/m^{2}s. The particle phase is Fluidized catalytic cracking(FCC)particles with a size of 59μm and material density is 1545 kg/m^3. The computational grid nodes are 141×351. The governing equations are solved by a finite volume method. The calculation domain is divided into a finite number of the control volumes. At main grid points placed in the center of the control volume, scalar quantity parameters such as the volume fraction of particles, density and turbulent kinetic energy are stored. A staggered grid arrangement is used and the velocity components are solved at the volume surfaces. The conservation equations are integrated in the space time and space.

3. SIMULATION RESULTS AND DISCUSSION

The parameters of the geometry, particle properties and computational mesh layout of CFB downer with initial conditions are shown in Figure 1. Initially the downer column was empty and the velocities of both phases were assumed to be zero.

Independent of grid size sensitivity is validated by the simulated particle concentration distribution(see Fig. 2) .Although the distribution of concentration exhibit the same trends along radial direction, the difference is also obvious, where the most significant discrepancy is located in the center region. An agreement results between medium and finer grid

size is found. Therefore, the medium grid size is used to reduce the computation times.

Figure 3 shows that comparison of simulated particle concentration with measured data under microgravity gravity, respectively. As we can see that predicted results under earth

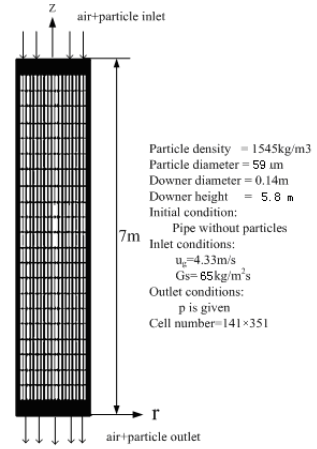

Fig.1 Scheme drawing of 2-D downer with inlet and initial conditions

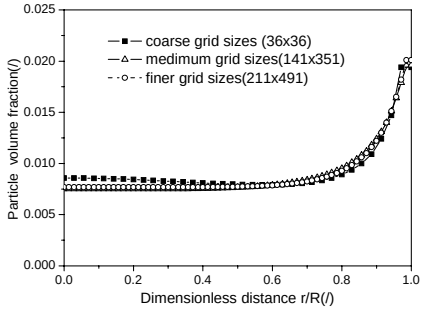

Fig.2 Independent of grid size sensitivity

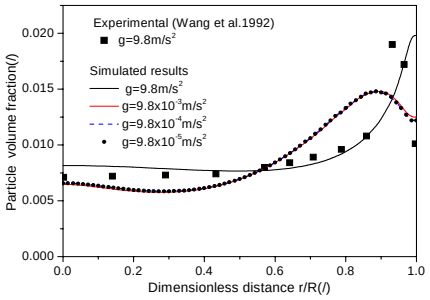

Fig.3 Comparison of simulated particle concentration with measured data under microgravity gravity

gravity are agreed well with the experimental data. The higher particle concentration phenomena located in near wall region with a peak value. Co-current two-phase flows with lower particle concentration and flat profiles are in accordance with measured results. Under microgravity conditions, all of peak values can be observed at aberrancy position, where it deviates from near wall region to some extents. Compared with simulated and measured data under earth gravity, they are smaller in the center region and they are larger in the near wall region. However, they are smaller in adjacent wall. In addition, their variation tendency is similar under different gravity. The alternation of peak value position will affect greatly the heat and mass transfer process, reaction time and designation of setup. The explanation is that peak value indicated the formation of maximum particle concentration. Particle-particle collision effects are dominant in turbulence flows. It takes a greater influence on gas-particle behavior due to the larger energy dissipation and the larger energy transportation. In fact, for the coexistence of single particle and clusters (higher particle concentration), energy will be transferred to particles and driven them break from clusters and move independently. Although particles are going to form the cluster in downer, cluster system is loose relatively due to gravity effects. With decreases of gravity value, gravity effects are reduced step by step. “Compacted cluster”, compared with “loose cluster” due to gravity effects prevents the particles from escaping.

As for the particle axial averaged velocity, simulated results under earth gravity are in good agreement with measured data (see Figure 4). But there is still a little discrepancy with experiments. The reason is that particle rotation and particle friction stress was neglected in particle temperature model. This shortcoming is further to be improved in the future research. Particle velocity of $g=9.8\times10^{-3}m/s^2$ gravity, it is the larger than any other gravities, which they have the same variation tendency. The larger velocity represents the smaller flow time or residence time. Hence, presented mathematical model and calculating code are validated by experimental data under gravity conditions. It may be used to predict gas-particle hydrodynamics in downer under microgravity conditions.

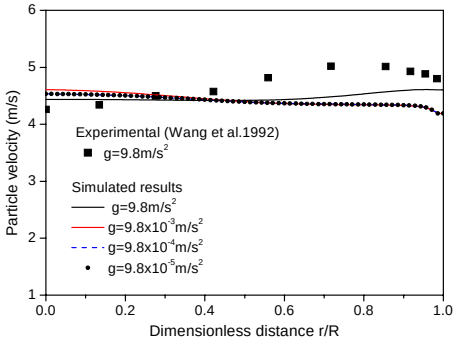

Fig.4 Comparison of simulated particle axial averaged velocity with measured data under microgravity gravity

Figure 5 shows the contour of particle concentration under microgravity environments. It can be seen that the all of the particle concentrations are higher near wall zone and are lower in center region in earth gravity. Under microgravity conditions, the coherent structure is differed from core-annular structure in a riser. Furthermore, all the distribution tendency of

particle concentration is similar, which have a uniformity flow structure. However, it decreases gradually to the center region.

Figure 6a and b show the simulated distribution of axial particle fluctuation velocity at the height section of 1.1m and 5.8m, respectively. Under earth gravity, at the inlet, two peaks can be found in Fig a. With the development of flow, fluctuation intensity is strengthened as well as fluctuation velocity is higher in the center and lower near wall region finally. When r/R is less

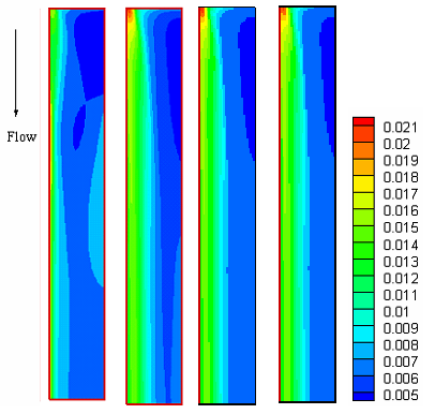

(a) (b) (c) (d)

Fig.5 Contour of particle concentration under microgravity environments (a: g=9.8 m/s^2; b: g= 9.8×10^{-3} m/s^2 ;c: g= 9.8×10^{-4} m/s^2 ;d: g= 9.8×10^{-5} m/s^2)

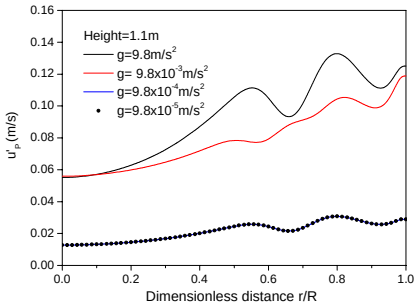

(a)

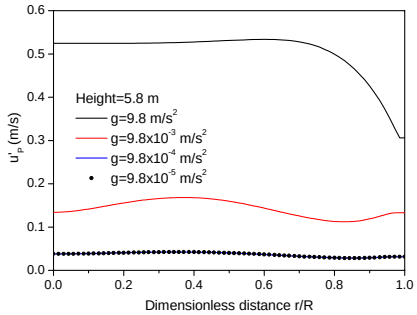

(b)

Fig.6 Profiles of axial particle fluctuation velocity under microgravity environments

than 0.7, fluctuation intensity profile is flat with higher value. Near wall region, fluctuation intensity profile is decreased with a greater velocity gradient. Under g=9.8×10^{-3}m/s^2 gravity, peaks are disappeared and the profiles are uniform gradually. Fluctuation velocity is lower in the center and is higher near wall region, which they are less than those of earth gravity. For g=9.8×10^{-4}m/s^2 and g=9.8×10^{-5}m/s^2 gravity, profiles are more uniform than others and their value are smaller than earth and g=9.8×10^{-3}m/s^2 gravity. Where a little higher value at near wall region than in the center one in inlet region and the same value are all the radial distribution.

Figure 7a and b show the simulated distribution of radial particle fluctuation velocity at the height section of 1.1m and 5.8m, respectively. At inlet height=1.1m position, one peak is observed for earth and g=9.8×10^{-3}m/s^2 gravity. In addition, the higher value is near wall region and the lower value in center region. The decreased gravity takes a little affects on distribution. For g=10^{-4}m/s^2 and g=9.8×10^{-5}m/s^2 gravity, they have the same value and variation tendency as well as their value is no changed along the radial distribution. Both of them are greatly smaller than those of earth and g=9.8×10^{-3}m/s^2 gravity. At height=5.7m position, profiles are more flat and uniform under microgravity than that of earth gravity. Decreased gravity decreased the particle dispersion, which is thoroughly differed from the up-flow dense gas-particle flows, which Liu et al.[6]drew a conclusion that the particle axial and radial fluctuation velocity under lunar-reduced gravity is greater than that of earth gravity in packed bed. Compared Fig.a to Fig. b, fluctuation velocity value in fully development region is larger than that of inlet region ones. Therefore, gravity condition and particle-particle collision are the important for dense gas-particle hydrodynamics.

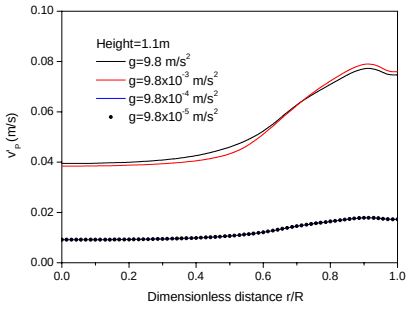

(a)

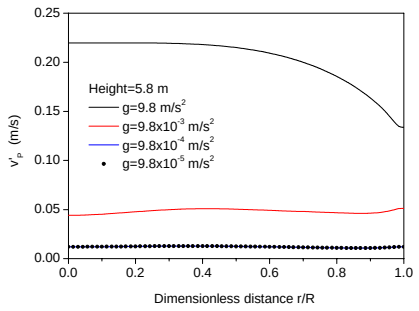

(b)

Fig.7 Profiles of radial particle fluctuation velocity under microgravity environments

Figure 8 shows that the simulated profiles of particle temperature at the height=5.8m. We can see that the particle temperature is lower near wall region and is higher in center region due to higher particle concentration with the greater energy decapitations under earth gravity. However, particle temperature near wall zone is slightly less than that of center region under microgravity conditions. This phenomena is thoroughly differ form that of earth condition, which indicates that the decreased particle temperature may be come from the decreases gravity. As mentioned above in Figure 7, particle dispersions are reduced by gravity decreasing and particles collisions. Furthermore, particle-particle collision can be weakened due to decreasing gravity. Compared Figure 7 to Figure 8, it can be seen that particle temperature is smaller than particle fluctuation both axial direction and radial direction. Figure 9 shows the contour of particle temperature under microgravity environments. Maximum particle temperature value is observed near wall region under earth gravity (see Fig.a) and no obvious maximum value can be found under microgravity condition. Furthermore, distributions of the whole field are entirely different. Compared to anisotropic flows structure under earth gravity, isotropic structures are easier to produce under microgravity conditions.

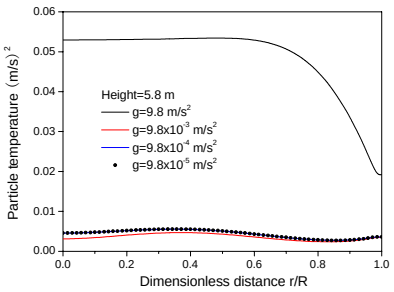

Fig.8 Profiles of particle temperature under microgravity environments

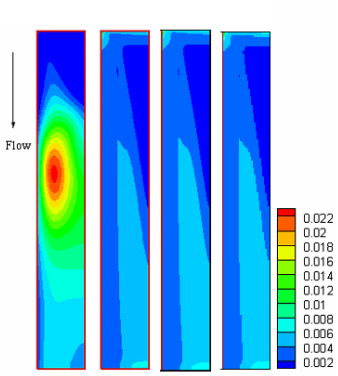

Fig.9 Contour of particle temperature under microgravity environments (a: g=9.8 m/s2; b: g= 9.8×10-3 m/s2 ;c: g= 9.8×10-4 m/s2 ;d: g= 9.8×10-5 m/s2)

Figure 10 shows profiles of axial-axial fluctuation velocity correlation of gas and particle. The gas-particle fluctuation velocity correlation is an important term in the second-order-moment two-phase turbulence model, which represents the turbulence interaction between the gas and particle Reynolds stresses. Under earth condition, it is approximately 3.0 times greater than microgravity. Thus, we can see than the decreasing gravity reduces the interaction between gas phase and particle phase. Comparison of Figure 6b, it can be seen that axial particle velocity fluctuation $u_p u_p$ is larger than those of $u_p u$ due to larger particle inertia and the larger particle turbulence diffusions.

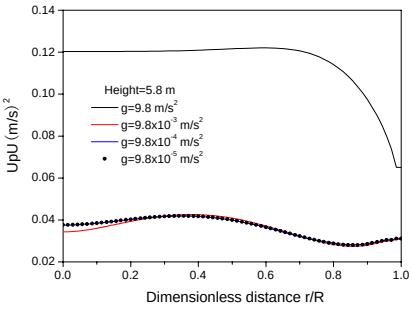

Fig.10 Profiles of axial-axial fluctuation velocity correlation of gas and particle

Figure 11 shows that the comparison of turbulent kinetic energy of gas and particle phase under microgravity environments. As we can see that particle kinetic energy is almost larger than gas and peak value is found at about the middle of downer under earth gravity(see Fig.a). As shown in Fig.b, particle kinetic energy energy is larger than that of gas at the outlet region. However, it is smaller than particle one at the middle and inlet region. In Fig.c and Fig.d, particle kinetic energy is smaller than that of gas at all the whole field section. Thus, the roles of particle and gas kinetic energy in particle-fluid system are alternated due to the decrease of gravity. Under earth gravity conditions, both particle and gas kinetic energy

are grater greatly than those of microgravity conditions.

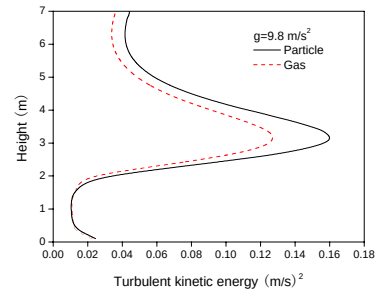

(a)

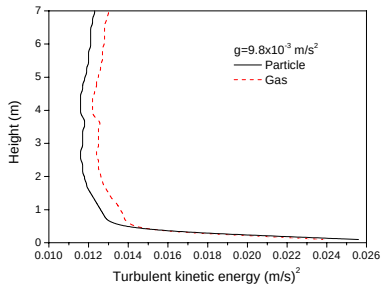

(b)

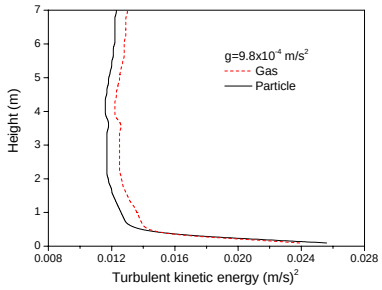

(c)

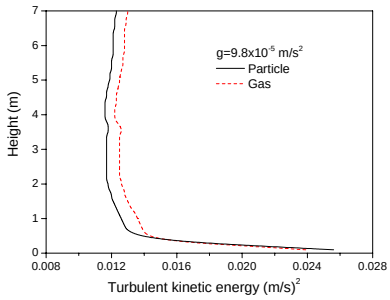

(d)

Fig.11 Comparison of turbulent kinetic energy of gas and particle phase under microgravity environments

4. CONCLUSIONS

The presented Euler-Euler two-fluid model closure with second-order-moment of dense gas-particle flows considered fully the anisotropy of gas-solid two-phase stresses and the interaction between two-phase stresses are fully considered by two-phase Reynolds stress model and the transport equation of two-phase stress correlation. Hydrodynamics and particle dispersion are predicted under microgravity environments. Under microgravity conditions, profiles of particle fluctuation velocity are more uniform than those of earth gravity. No obvious peaks of particle concentration are formed in the flows field. Decrease of gravity is easier to produce the isotropic gas-particle two-phase turbulence structure. Particle fluctuation intensity, particle temperature and axial-axial fluctuation velocity correlation of gas and particle are reduced. The roles of particle kinetic energy and gas kinetic energy in two-phase system are alternated due to the decrease of gravity. Under earth gravity conditions, both particle and gas kinetic energy are grater greatly than microgravity environments.

ACKNOWLEDGEMENT

We sincerely appreciate the Key Younger Teacher Project of Dalian Maritime University Grants 017025 and the Projects of National Natural Science Foundation of China under the Grants 50606026.

REFERENCES

[1] Eckart, P., 1999, "The Lunar Base Handbook-an Introduction to Lunar Base Design, Development, and Operations. McGraw-Hill Companies, Inc., New York., pp. 851-864..

[2] David, K. B., Scott, R.L., 2005, "Simulating Lunar Habitats and Activities to Derive System Requirements", 1st Space Exploration Conference: continuing the voyage of discovery. AIAA, pp. 2708-2720.

[3] Lyubimov, D. V., Lyubimova, T. P., Straube, A. V., 2005, "Accumulation of Solid Particles in Convective Flows", Microgravity Science and Technology, 16,pp.1-5.

[4] Lyubimov, Y .A., Ichiro, U., Hiroshi, K., 2007, "Effect of Shape of HZ Liquid Bridge on Particle Accumulation Structure (PAS)", Microgravity Science and Technology,19, pp. 3-9.

[5] Noreen, K. M.,2008, "The Lunar Environment: Determining the Health Effects of Exposure to Moon Dusts", Acta Astronautica, 63, 1006-1014.

[6] Liu, Y., Li, G. H., Jiang, L. X., 2010, "Hydrodynamic Behavior of Dense Gas Particle Flows under the Reduced Gravity Conditions", Acta Astronautica, DOI: 10.1016/j.actaastro.2010.02.023

[7] Srivastava, A., Agrawal, K., Sundaresan, S., Reddy. S. B., 1998, "Dynamics of Gas-Particle Flow in Circulating Fluidized Beds", Powder Technology, 100, 173-182.

[8] Lehner, P., Wirth, K.E., 1999, "Characterization of the Flow Pattern in a Downer Reactor", Chemical Engineering Science, 54, pp. 5471-5483.

[9] Cheng, Y., Guo, Y. C., Wei, F., 1999, "Modeling the Hydrodynamics of Downer Reactors Based on Kinetic Theory", Chemical Engineering Science, 54, pp. 2019-2027.
[10] Liu, W., Luo, K. B., Zhu, J. X., Beeckmans, J. M., 2001, "Characterization of High-Density Gas–Solids Downward Fluidized Flow", Powder Technology, 115, pp. 27-35.
[11] Zhang, X, Zhou, L. X., 2003, "Simulation of Gas-Particle Channel Flows using a Two-Fluid Particle-Wall Collision Model Accounting for Wall Roughness", Proc. 4th ASME/JSME Joint Fluid Eng. Conf. Hawaii, USA, FEDSM2003-45750.
[12] Li, S. G., Lin, W. G., Yao, J. Z., 2004, "Modeling of the Hydrodynamics of the Fully Developed Region in a Downer Reactor", Powder Technology, 145, pp. 73-81.
[13] Lu, X. S., Li, S. G., Li, H. Z., 2005, "Flow structures in the Downer Circulating Fluidized Bed", Chemical Engineering Journal, 112, pp. 23-31.
[14] Lu, H.L., Gidaspow, D., 2003, "Hydrodynamics of Binary Fluidization in a Riser: CFD Simulation using Two Granular Temperatures", Chemical Engineering Science, 58, pp. 3777-3792.
[15] Luo, B. L., Yan, D., Zhu, J., 2007, "Characteristics of Gas–Solid Mass Transfer in a Cocurrent Downflow Circulating Fluidized Bed Reactor", Chemical Engineering Journal, 132, pp. 9-15.
[16] Wu, C. N., Cheng, Y., Jin, Y., 2008, "Modeling the Hydrodynamics in a Coupled High Density Downer-to-Riser Reactor", Powder Technology, 181, pp. 255-265.
[17] He, Y.R., Deen, N.G., Kuipers, J.A.M., 2009, "Gas-Solid Turbulent Flow in a Circulating Fluidized Bed Riser: Numerical Study of Binary Particle Systems", Industrial and Engineering Chemistry Research, 48, pp. 8098-8108.
[18] Lun, C. K., Savage, S. B., Jeffrey, D. J., 1984, "Kinetic Theories for Granular Flow: Inelastic Particles in Coquette Flow and Slightly Inelastic Particles in a General Flow Field", J. Fluid Mechanics, 140, pp. 223-256
[19] Ding, J., Gidaspow, D., 1990, "A Bubbling Fluidization Model with Kinetic Theory of Granular Flow". AICHE. Journal, 36, pp. 523-538.
[20] Savage, S. B., 1998, "Analysis of Slow High-Concentration Flows of Granular Materials", J. Fluid Mechanics, 377, pp. 1-26.
[21] Gidaspow, D., 1994, "Multiphase Flow and Fluidization: Continuum and Kinetic Theory Description", New York. Academic Press, pp. 65-78.
[22] Sinclair, J. L., Jackson, R., 1989, "Gas-Particle Flow in a Vertical Pipe with Particle-Particle Interaction", AICHE. Journal., 35, pp. 1473-1486.
[23] Bolio, E. J., Yasuna, J. A., Sinclair, J. L., 1995, "Dilute Turbulent Gas-Solid Flow in Riser with Particle-Particle Interactions", AICHE Journal., 41, pp. 1375-1388.
[24] Lu, H. L., Liu, W. T., Bie, R. S., Gidaspow, D., 2000, "Kinetic theory of fluidized binary granular mixtures with unequal granular temperature", Physica A .284, pp. 265-276.
[25] Wang, S. Y., Shen, Z. H., Lu, H. L., 2008, "Numerical Predictions of Flow Behavior and Cluster Size of Particles in Riser with Particle Rotation Model and Cluster-Cased Approach", Chemical Engineering Science, 63, pp. 4116-4125.
[26] Zhou, L. X., 1993, "Theory and Numerical Simulation Modeling of Turbulent Gas-Particle Flows and Combustion", Beijing, Science Press and Florida, CRC Press., pp. 13-21.
[27] Zhou, L. X., Chen, T., 2001, "Simulation of Strongly Swirling Gas-Particle Flows using USM and k-ε-kp Two-Phase Turbulence Models", Powder Technology, 114, pp. 1-11.
[28] Zhou, L. X., Liao, C. M., Chen, T., 1994, "A Unified Second-Order-Moment Two-Phase Turbulence Model for Simulating Gas-Particle Flows", ASME. 185, 307-313.
[29] Liu, Y., Zhou, L. X., Xu, C. X., 2009, "Large-eddy Simulation of Swirling Gas-Particle Flows using a USM Two-Phase SGS Stress Model", Powder Technology, 198, pp. 183-188.
[30] Cheng, Y., Guo,Y. C., Wei, F., 1999, "Modeling the Hydrodynamics of Downer Reactors Based on Kinetic Theory", Chemical Engineering Science, 54, pp. 2019-2027
[31] Wen, C. Y., Yu, Y. H., 1966, "Mechanics of Fluidization", Chem. Eng. Prog.Symp, 62, pp.100-108.
[32] Mohanarangam, K., Tu, J. Y., 2007, "Two-Fluid Model for Particle-Turbulence Interaction in a Backward-Facing Step", AICHE. J, 53, pp. 2254-2271.
[33] Wang, Y., Bai, D.R., Jin, Y., 1992, "Hydrodynamics of Cocurrent Downflow Circulating Fluidized Bed(CDCFB)", Powder Technology, 70, pp. 271-275.